Transmission spectra of sausage-like microresonators

Ming-Yong Ye,* Mei-Xia Shen, and Xiu-Min Lin

Fujian Provincial Key Laboratory of Quantum Manipulation and New Energy Materials, College of Physics and Energy, Fujian Normal University, Fuzhou 350007, China

*myye@fjnu.edu.cn

Abstract: We experimentally develop a sausage-like microresonator (SLM) by making two microtapers on a single-mode fiber, and study whispering-gallery modes (WGMs) in SLMs with different lengths. The transmission spectra from 1530 nm to 1550 nm of several SLMs are presented and SLMs with different lengths are shown to have different transmission features. The maximal Q factor observed in the SLMs is $3.8 * 10^7$. For comparison, the transmission spectrum of a fiber cylinder microresonator is given and the maximal Q factor achieved in the fiber microcylinder resonator is $1.7 * 10^7$. The strain tuning of the SLM is also demonstrated.

OCIS codes: (060.2340) Fiber optics components; (140.3945) Microcavities; (230.3990) Micro-optical devices.

References and links

1. B. Peng, Ş. K. Özdemir, F. Lei, F. Monifi, M. Gianfreda, G. L. Long, S. Fan, F. Nori, C. M. Bender, and L. Yang, "Parity-time-symmetric whispering-gallery microcavities," Nat. Phys. **10**, 394–398 (2014).
2. L. Chang, X. Jiang, S. Hua, C. Yang, J. Wen, L. Jiang, G. Li, G. Wang, and M. Xiao, "Parity-time symmetry and variable optical isolation in active-passive-coupled microresonators," Nat. Photon. **8**, 524–529 (2014).
3. C. Dong, V. Fiore, M. C. Kuzyk, and H. Wang, "Optomechanical dark mode," Science **338**, 1609–1613 (2012).
4. Y. S. Park, A. K. Cook, and H. Wang, "Cavity qed with diamond nanocrystals and silica microspheres," Nano Lett. **6**(9), 2075–2079 (2006).
5. C.-H. Dong, Z. Shen, C.-L. Zou, Y.-L. Zhang, W. Fu, and G.-C. Guo, "Brillouin-scattering induced transparency and non-reciprocal light storage," Nat. Commun. **6**, 6193 (2015).
6. M. Cai, O. Painter, K. J. Vahala, and P. C. Sercel, "Fiber-coupled microsphere laser," Opt. Lett. **25**, 1430–1432 (2000).
7. Y.-Z. Huang, K.-J. Che, Y.-D. Yang, S.-J. Wang, Y. Du, and Z.-C. Fan, "Directional emission InP/GaInAsP square-resonator microlasers," Opt. Lett. **33**(19), 2710–2712 (2008).
8. L. Shao, X. F. Jiang, X. C. Yu, B. B. Li, W. R. Clements, F. Vollmer, W. Wang, Y. F. Xiao, and Q. Gong, "Detection of single nanoparticles and lentiviruses using microcavity resonance broadening," Adv. Mater. **25**, 5616–5620 (2013).
9. J. Zhu, S. K. Ozdemir, Y.-F. Xiao, L. Li, L. He, D.-R. Chen, and L. Yang, "On-chip single nanoparticle detection and sizing by mode splitting in an ultrahigh-q microresonator," Nat. Photon. **4**, 46–49 (2010).
10. F. Vollmer and S. Arnold, "Whispering-gallery-mode biosensing: label-free detection down to single molecules," Nat. Meth. **5**, 591–596 (2008).
11. B.-B. Li, W. R. Clements, X.-C. Yu, K. Shi, Q. Gong, and Y.-F. Xiao, "Single nanoparticle detection using split-mode microcavity Raman lasers," Proc. Natl. Acad. Sci. USA **111**(41), 14657–14662 (2014).
12. M. Sumetsky, "Mode localization and the Q-factor of a cylindrical microresonator," Opt. Lett. **35**(14), 2385–2387 (2010).
13. M. Sumetsky, and Y. Dulashko, "Radius variation of optical fibers with angstrom accuracy", Opt. Lett. **35**(23), 4006–4008 (2010).
14. X. Zhang, Z. Ma, H. Yu, X. Guo, Y. Ma, and L. Tong, "Plasmonic resonance of whispering gallery modes in an Au cylinder," Opt. Express **19**(5), 3902–3907 (2011).

#245441 Received 7 Jul 2015; revised 3 Sep 2015; accepted 16 Sep 2015; published 23 Sep 2015

15. M. L. Gorodetsky, A. A. Savchenkov, and V. S. Ilchenko, "Ultimate Q of optical microsphere resonators," Opt. Lett. **21**(7), 453–455 (1996).
16. T. J. Kippenberg, S. M. Spillane, D. K. Armani, and K. J. Vahala, "Fabrication and coupling to planar high-Q silica disk microcavities," Appl. Phys. Lett. **83**(4), 797–799 (2003).
17. F. Bo, S. H. Huang, Ş. K. Özdemir, G. Zhang, J. Xu, and L. Yang, "Inverted-wedge silica resonators for controlled and stable coupling," Opt. Lett. **39**, 1841–1844 (2014).
18. J. Lin, Y. Xu, Z. Fang, M. Wang, J. Song, N. Wang, L. Qiao, W. Fang, and Y. Cheng, "Fabrication of high-Q lithium niobate microresonators using femtosecond laser micromachining," Sci. Rep. **5**, 8072 (2015).
19. D. K. Armani, T. J. Kippenberg, S. M. Spillane, and K. J. Vahala, "Ultra-high-q toroid microcavity on a chip," Nature **421**, 925–928 (2003).
20. X. F. Jiang, Y. F. Xiao, C. L. Zou, L. He, C. H. Dong, B. B. Li, Y. Li, F. W. Sun, L. Yang, and Q. Gong, "Highly unidirectional emission and ultralow-threshold lasing from on-chip ultrahigh-Q microcavities," Adv. Mater. 24, OP260–OP264 (2012).
21. M. Pöllinger, D. O'Shea, F. Warken, and A. Rauschenbeutel, "Ultrahigh-q tunable whispering-gallery-mode microresonator," Phys. Rev. Lett. **103**(5), 053901 (2009).
22. M. Ding, G. S. Murugan, G. Brambilla, and M. N. Zervas, "Whispering gallery mode selection in optical bottle microresonators," Appl. Phys. Lett. **100**(8), 081108 (2012).
23. G. Gu, C. Guo, Z. Cai, H. Xu, L. Chen, H. Fu, K. Che, M. Hong, S. Sun, and F. Li, "Fabrication of ultraviolet-curable adhesive bottle-like microresonators by wetting and photocuring," Appl. Opt. **53**, 7819–7824 (2014).
24. A. Lee, T. Mills, and Y. Xu, "Nanoscale welding aerosol sensing based on whispering gallery modes in a cylindrical silica resonator," Opt. Express **23**(6), 7351–7365 (2015).
25. V. Zamora, A. Díez, M. V. Andrés, and B. Gimeno, "Interrogation of whispering-gallery modes resonances in cylindrical microcavities by backreflection detection," Opt. Lett. **34**(7), 1039–1041 (2009).
26. T. A. Birks, J. C. Knight, and T. E. Dimmick, "High-resolution measurement of the fiber diameter variations using whispering gallery modes and no optical alignment," IEEE Photon. Technol. Lett. **12**(2), 182–183 (2000).
27. A. W. Poon, R. K. Chang, and J. A. Lock, "Spiral morphology-dependent resonances in an optical fiber: effects of fiber tilt and focused Gaussian beam illumination," Opt. Lett. **23**(14), 1105–1107 (1998).
28. C. Yin, J. Gu, M. Li, and Y. Song, "Tunable high-Q tapered silica microcylinder filter," Chin. Opt. Lett. **11**(8), 082302 (2013).
29. V. Kavungal, L. Bo, Q. Wu, M. Teng, C. Yu, G. Farrell, and Y. Semenova, "Study of whispering gallery modes in a cylindrical microresonator excited by a tilted fiber taper," Proc. SPIE **9157**, 91578N (2014).
30. F. Luan, E. Magi, T. Gong, I. Kabakova, and B. J. Eggleton, "Photoinduced whispering gallery mode microcavity resonator in a chalcogenide microfiber," Opt. Lett. **36**(24), 4761–4763 (2011).
31. M. Sumetsky, and J. M. Fini, "Surface nanoscale axial photonics," Opt. Express, **19**(27), 26470–26485 (2011).
32. H. Zhu, I. M. White, J. D. Suter, M. Zourob, and X. Fan, "Integrated refractive index optical ring resonator detector for capillary electrophoresis," Anal. Chem. **79**(3), 930–937 (2007).
33. Y. Dong, X. Jin, and K. Wang, "Packaged and robust microcavity device based on a microcylinder-taper coupling system," Appl. Opt. **54**(13), 4016–4022 (2015).
34. G. S. Murugan, M. N. Petrovich, Y. Jung, J. S. Wilkinson, and M. N. Zervas, "Hollow-bottle optical microresonators," Opt. Express **19**(21), 20773–20784 (2011).

1. Introduction

Over the last decade, optical dielectric microresonators supporting whispering-gallery modes (WGMs) have attracted increasing research interest. Due to their high quality (Q) factor and very small mode volume, WGM microresonators hold great potential in fundamental physics and real applications [1–11]. The high Q of WGMs results from the fact that light is confined by continuous total internal reflection meanwhile the leakage out of the cavity is small. So far, WGM microresonators with various geometries including microcylinders [12–14], microspheres [15], microdisks [16–18], microtoroids [19, 20], and microbottles [21–23] have been investigated. Among them, microcylinder resonators can be made very easily from optical fibers and have received some attentions [13, 24–29]. However, the reported Q factor of fiber microcylinder resonators is about 10^5 [24, 25, 29], which is poor compared to other WGM microresonators such as silica microspheres (larger than 10^8). Through modifying the shape of a microcylinder resonator [30], the Q factor may be improved. Surface nanoscale axial photonics (SNAP) platform is recently introduced for creating high Q microresonators [31]. SNAP devices with effective nanoscale variation of the fiber radius and/or the equivalent variation of refractive index are reported to have Q factor of magnitude 10^7 [31].

#245441 Received 7 Jul 2015; revised 3 Sep 2015; accepted 16 Sep 2015; published 23 Sep 2015

In this paper, another way to modify fiber microcylinder resonators is put forward. The method is to make two microtapers on a fiber, and between them is still a length of smooth fiber (see Fig. 1). The shape of the achieved geometry is like a sausage, so it will be called a sausage-like microresonator (SLM) hereafter. Mode characteristics of SLMs with different lengths will be studied. To show the difference between SLMs and microcylinder resonators, experimental results on a fiber microcylinder will be also given. Finally an experimental result on the strain tuning of the SLM will be presented.

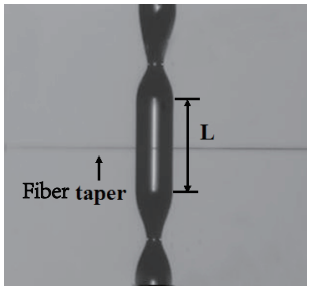

Fig. 1. A sausage-like microresonator (SLM). The picture is taken from a monitoring CCD camera. The arrow is used to point out the position of the fiber taper, which is perpendicular to the microresonator. The letter L represents the length of the smooth part in the SLM.

2. Fabrication and experimental setup

SLMs were fabricated from a 125 μm-diameter single-mode optical fiber, and the method we used was a kind of heat-and-pull method [21]. A single-mode optical fiber with the plastic coating removed was first cleaned by alcohol. It was then kept vertical in a precise three-dimensional adjustment bracket by attaching a small weight in the lower end of the fiber. The fiber was heated by a CO_2 laser on two different points, respectively. The positions of the heated points were controlled by the adjustment bracket that could move the fiber up and down. Under the gravity, the heated points were pulled to become two microtapers so that a SLM was fabricated. There is still an unheated part in the center of the microresonator whose length, represented by the letter L, will be called the length of the SLM. The lengths of the SLMs were estimated from a monitoring CCD camera attached to a microscope.

The experimental excitation of WGMs in microresonators was accomplished through evanescent wave coupling with a fiber taper [6], whose waist diameter was about 2 μm. Basic experimental setup was as following. One end of the fiber taper was connected to a 1550 nm band tunable laser with the linewidth smaller than 200 kHz. The fiber taper and the microresonator were placed on two translation stages with a resolution of 20 nm, respectively. By controlling the translation stages we could adjust the air gap between the fiber taper and the microresonator. The other end of the fiber taper was connected to a 125 MHz low-noise optical detector, which was then linked to a digital oscilloscope to obtain transmission spectra. All transmission spectra were obtained with the fiber taper perpendicular to the microresonator (see Fig. 1).

3. Transmission spectrum of a fiber microcylinder

For reference and comparison, we first give our experimental result on a fiber microcylinder. The microcylinder was made of a 125 μm-diameter single-mode fiber with a total length of 9.5 cm. On one end of the fiber microcylinder, a 2 cm-long plastic coating was removed and the end was cut flat. The section of the fiber with the plastic coating removed was then cleaned by alcohol. The fiber taper was placed on the part without plastic coating to excite WGMs,

#245441 Received 7 Jul 2015; revised 3 Sep 2015; accepted 16 Sep 2015; published 23 Sep 2015

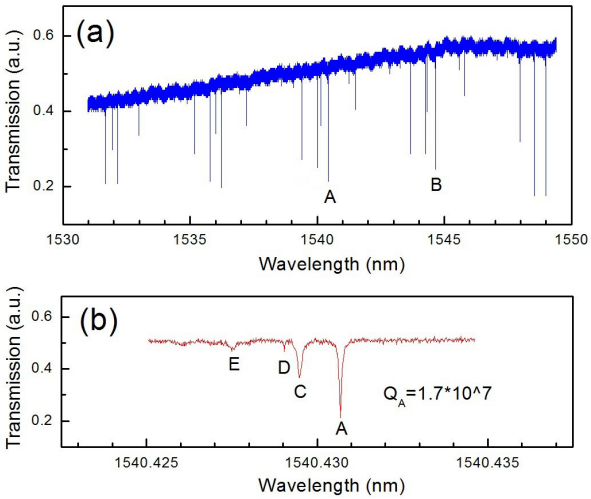

Fig. 2. (a) Transmission spectrum of a fiber microcylinder. (b) An amplification of mode A.

where the distance between the fiber taper and the end of the microcylinder was 1.2 cm. Figure 2(a) shows the observed transmission spectrum from 1530 nm to 1550 nm with the fiber taper not in contact with the microcylinder. The modes A and B appear to have the same radial order but successive angular orders. The free spectral range (FSR) is clear, which is 4.22 nm measured from the difference between the resonance wavelengths of modes A and B. The theoretical value of FSR is $\lambda^2/(\pi \mathrm{Dn})$=4.21 nm where we have set the refractive index n=1.44, the fiber diameter D=125 μm and λ=1543 nm. Therefore the measured FSR is consistent with the theoretical prediction. Figure 2(b) shows an amplification of mode A, whose Q factor is $1.7 * 10^7$. The modes C, D and E in Fig. 2(b) are too close to mode A and can not be seen from the spectrum in Fig. 2(a), which appear to be modes with higher radial orders than mode A.

The Q factor ($Q \sim 10^7$) we achieved is much higher than the reported before in fiber microcylinders ($Q \sim 10^5$) [24,25,29], and is very close to the theoretical prediction by Sumetsky [12]. According to the prediction of Sumetsky, a low-absorption fiber microcylinder can support localized high-Q (10^7) WGMs with the mode function's width along the cylinder axis being about 2 mm [12]. Therefore, these high-Q modes can not be observed if the fiber taper is placed very close to the end of the microcylinder. That the fiber taper is placed too close to the end may be the possible reason why there is no Q factor of 10^7 ever reported. In addition, some reported experiments on fiber microcylinder are done with the fiber taper in contact with the microcylinder [24, 26, 29], which can also reduce the observed Q factors. It is noted that Q factors of 10^6 in liquid filled capillaries [32] and 10^7 in heat-treated fiber microcylinders [33] are reported, but they are not the same kind of fiber microcylinder resonator as that we studied.

4. Transmission spectra of SLMs

In this section, we will give our experimental results on SLMs with several different lengths. As it is mentioned in the previous section, the mode function's width along the cylinder axis of a localized high-Q WGM in a fiber microcylinder is about 2 mm [12]. Therefore, it can be imagined that when the length of a SLM is much larger than 2 mm and the fiber taper is placed on the center of the SLM to excite WGMs, the localized WGMs will not be affected by the two microtapers on the SLM. Figure 3(a) is the observed transmission spectrum of a SLM with the

#245441 Received 7 Jul 2015; revised 3 Sep 2015; accepted 16 Sep 2015; published 23 Sep 2015

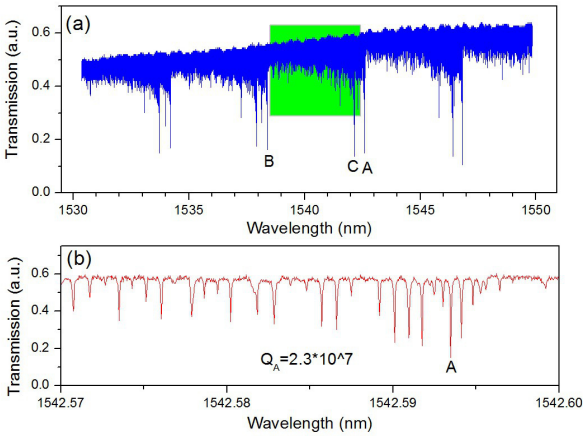

Fig. 3. (a) Transmission spectrum of a SLM with its length L=7.5 mm. (b) An amplification of mode A.

length L=7.5 mm, with the fiber taper placed on the center of the SLM and not in contact with the SLM. It can be seen that the FSR is clear and it is 4.22 nm measured from the difference between the resonance wavelengths of modes A and B, which is the same as the measured FSR of the fiber microcylinder in the previous section. Figure 3(b) is an amplification of mode A, whose Q factor is $2.3 * 10^7$. The efficiently excited modes like A, B and C in Fig. 3(a) appear to be localized high-Q WGMs supported by the fiber cylinder, and the existence of the two microtapers on the SLM has no effect on them, since the length of the SLM is much larger than the width of the mode function. The resonance wavelengths of these efficiently excited localized high-Q modes in Fig. 3(a) are different from those in the transmission spectrum of the fiber microcylinder in Fig. 2(a), the reason can be that the polarizations of the excitation laser in two experiments are different [26].

It is known that in addition to localized high-Q WGMs, a fiber microcylinder can also support spiral modes that have resonance wavelength smaller than the corresponding localized WGMs [27]. The spiral modes have non-zero wave vectors along the cylinder axis so that they can propagate along the cylinder axis. Similar to bottle microresonators [21], the two microtapers on the SLM provide two barriers for spiral modes, so that they are confined to move between the two microtapers and thus can be excited. This is the reason why between modes A and B the number of modes is huge (indicated by green background in Fig. 3(a)). These modes are confined spiral modes except for some localized modes like mode C.

The confined spiral modes with green background between modes A and B in Fig. 3(a) show an interesting global feature that spiral modes near the mode A are more effectively excited than those near the mode B. The feature can be understood qualitatively as follows [25]. The laser light propagating in the fiber taper is not a plane wave, but it can be written as a superposition of many plane waves and some of the plane waves have non-zero wave vectors along the SLM axis. Note that the fiber taper is placed perpendicular to the SLM. Therefore, in the plane wave superposition of the laser light, roughly speaking the larger the wave vector along the SLM axis a plane wave has, the smaller the amplitude of the plane wave is. The confined spiral modes are mainly excited by plane waves that have non-zero wave vectors along the SLM axis. For the spiral modes focused here (indicated by green background in Fig. 3(a)), the spiral modes near mode B have larger non-zero wave vectors along the SLM axis than those near mode A [27], so that the intensity of the plane waves used to excite spiral modes near mode B will be smaller

#245441 Received 7 Jul 2015; revised 3 Sep 2015; accepted 16 Sep 2015; published 23 Sep 2015

than the intensity of the plane waves used to excite spiral modes near mode A. Therefore, spiral modes (with green background) near the mode A are more effectively excited than those near the mode B.

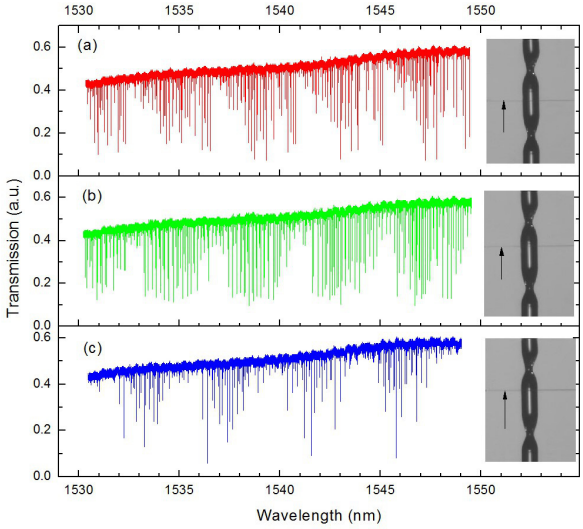

Fig. 4. Transmission spectra of a SLM with its length L=200 μm. In the insets on the right, arrows are used to point out the positions of the fiber taper.

Figure 4 shows the experimental results on a SLM with its length L=200 μm. It gives the observed transmission spectra with the fiber taper placed at several different positions along the SLM. In the experiment, the fiber taper is not in contact with the SLM and the maximal Q factor observed is $2.8 * 10^7$. There are four main features about the spectra. (1) The number of modes that are efficiently excited in Fig. 4 is larger than that in Fig. 3(a) where only the localized WGMs like A, B and C are efficiently excited. This is because the length of the SLM (200 μm) is now much smaller than the spatial width of localized high-Q WGMs (2 mm) supported by a fiber microcylinder, so that it is not proper to divide modes into localized WGMs and confined spiral modes in a clear way as in the SLM with the length L=7.5 mm. (2) Amplifying any mode in Fig. 4 will not give more dips, which is different from the result on the SLM with the length L=7.5 mm, where more than 10 modes (dips) can be found within 0.02 nm as shown in Fig. 3(b). It can be understood from the fact that when the length of the SLM becomes shorter the movement of light along the SLM axis will be more confined. Therefore, similar to Fabry-Pérot cavities the mode density will decrease as the length of the SLM decreases. (3) In any spectrum in Fig. 4, the resonance wavelengths of the excited modes are grouped into several bands. In the band gaps, the modes are not excited or not efficiently excited. Compare the spectra in Figs. 4(a)–4(c), it can be found that the positions of the band gaps are different. This is due to the fact that the mode functions have nodes along the SLM axis, which is similar to an electron moving in a harmonic potential in one dimension where different stationary states have different node positions. When the fiber taper is placed on the node of a mode function, the mode will not be efficiently excited. (4) Figure 4(c) shows a cleaner spectrum than Figs. 4(a) and 4(b). This is because Fig. 4(c) is obtained by placing the fiber taper very close to the microtaper on the SLM, and the microtaper increases the loss of some modes. The spectral cleaning is similar to that in bottle microresonators [22, 34].

Figure 5(a) shows the transmission spectrum of a SLM with its length L=83 μm. The fiber

#245441 Received 7 Jul 2015; revised 3 Sep 2015; accepted 16 Sep 2015; published 23 Sep 2015

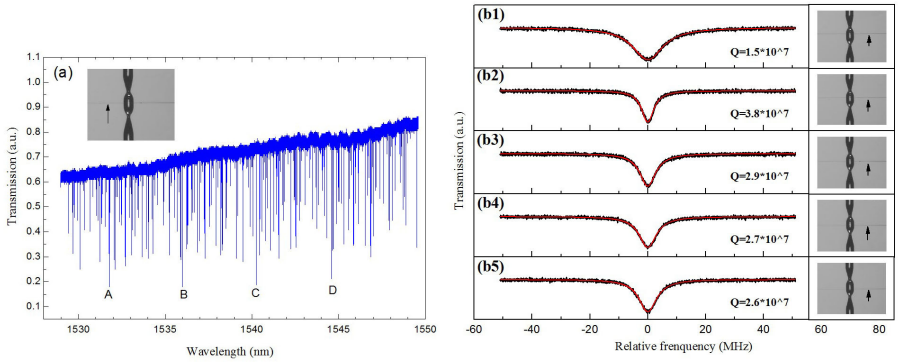

Fig. 5. (a) Transmission spectrum of a SLM with its length L=83 μm and (b) measurement of Q factors at different positions along the SLM. The red lines are Lorentz fittings. In the insets, arrows are used to show the positions of the fiber taper.

taper is placed at the center of the SLM and is not in contact with the SLM. The modes A, B, C and D appear to have the same radial order but successive angular orders. The spectrum has its own feature that there are no clear "band gaps" compared to those in Fig. 4. This is because the length of the SLM is further reduced so that the mode functions are more confined along the SLM axis, which can then increase the coupling to the the fiber taper. The Q factors are also measured through a fine sweeping of the laser with the fiber taper placed on several positions along the SLM, and the results are shown in Figs. 5(b1)–5(b5). In Fig. 5(b1) the fiber taper is placed close to the upper microtaper on the SLM, and in Fig. 5(b5) the fiber taper is placed close to the lower microtaper on the SLM. The experimental result shows that larger Q factors are observed when the fiber taper is placed near the center of the SLM. The maximal Q factor observed is $3.8 * 10^7$, which is also the maximal Q factor we observed in these three SLMs.

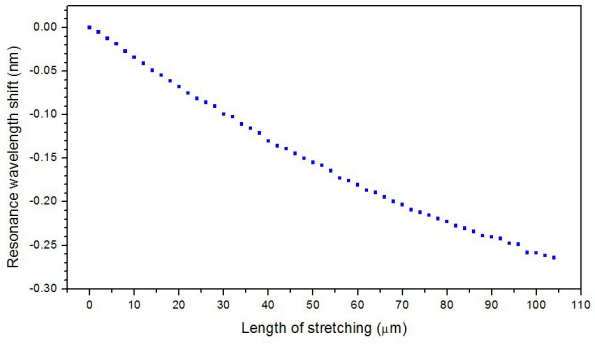

Fig. 6. Experimental result on the strain tuning of a SLM with the length L=178 μm.

5. Tunability of resonance wavelength

Similar to fiber microbottles [21], the resonance wavelengths of SLMs can be tuned by straining. To demonstrate strain tuning, one side of the SLM was fixed and the other side was connected to a stage with differential adjusters. The fine adjuster of the stage has a vernier scale with 1 μm graduations, and the coarse adjuster has a vernier scale with 10 μm graduations.

#245441 Received 7 Jul 2015; revised 3 Sep 2015; accepted 16 Sep 2015; published 23 Sep 2015

The transmission spectra of a SLM with the length L=178 μm were obtained through a fine sweeping of the laser with a range of 0.3 nm, where the fiber taper was placed near the center of the SLM and was not in contact with the SLM. A mode with the resonance wavelength about 1550 nm was focused. Figure 6 shows its resonance wavelength shift with a fine stretching step of 2 μm, and the resonance wavelength experiences a blue shift of 0.26 nm when the SLM is stretched by a length of 100 μm. The SLM was finally stretched with the coarse adjuster to test how long it can be stretched before damage. It was found that one microtaper on the SLM was broken after stretched a total length about 400 μm (including the previous fine stretching length).

6. Discussion and summary

A fiber microcylinder can support localized WGMs and delocalized spiral modes. When two micotapers are made on a fiber microcylinder to form a SLM, spiral modes will be confined to move between the two microtapers and thus become localized. In some sense SLMs are similar to microbottles, where light is confined to move between two turning points along the resonator axis. Fiber microbottles can be regarded as special SLMs with the length L=0. Compared to fiber microcylinders and microbottles, SLMs can support more localized modes and the mode density is related to its length. The large mode density combined with the strain tunability of the SLM makes it more convenient to obtain a mode with a desired resonance wavelength, which is usually necessary in cavity QED study.

In summary, a sausage-like microresonator (SLM) is demonstrated. Transmission spectra from 1530 nm to 1550 nm of three SLMs are presented. It is found that SLMs with different lengths can show different transmission features. The maximal Q factor observed in SLMs is $3.8 * 10^7$. The transmission spectrum of a fiber microcylinder is also presented. The observed maximal Q factor of the fiber microcylinder is $1.7 * 10^7$. The shape of SLMs makes them easy to tune the resonance wavelength through stretching and the tunability has been experimentally demonstrated.

Acknowledgments

We would like to thank Chun-Hua Dong for helpful comments. This work was supported by the National Natural Science Foundation of China (Grant Nos. 61275215), the National Fundamental Research Program of China (Grant No. 2011CBA00203) and Fujian Provincial College Funds for Distinguished Young Scientists (Grant No. JA14070).

#245441 Received 7 Jul 2015; revised 3 Sep 2015; accepted 16 Sep 2015; published 23 Sep 2015